Ain Shams Engineering Journal (2010) 1, 49–58

Ain Shams University

Ain Shams Engineering Journal

www.elsevier.com/locate/asej
www.sciencedirect.com

ELECTRICAL ENGINEERING

Neural predictive controller of a two-area load frequency control for interconnected power system

Ahmed M. Kassem

Control Technology Dep., Industrial Education College, Peni-Suef University, Egypt

Received 17 April 2010; accepted 6 May 2010
Available online 16 November 2010

KEYWORDS
Neural predictive control;
Model predictive control;
Fuzzy logic control;
Two area load frequency control

Abstract The present paper investigates the load-frequency control (LFC) for improving power system dynamic performance over a wide range of operating conditions. This study proposed design and application of the neural network model predictive controller (NN-MPC) on two-area load frequency power systems. Neural network model predictive control (NN-MPC) combines reliable prediction of neural network with excellent performance of model predictive control using nonlinear Levenberg–Marquardt optimization. The controller used the local power area error deviation as a feedback signal. To validate the effectiveness of the proposed controller, two-area power system is simulated over a wide range of operating conditions and system parameters change. Further, the performance of the proposed controller is compared with a fuzzy logic controller (FLC) through simulation studies. Obtained results demonstrate the effectiveness and superiority of the proposed approach.

1. Introduction

Large-scale power systems are normally composed of interconnected subsystems. The connection between the control areas is done using tie lines. Each area has its own generator or multigenerators and it is responsible for its own load and scheduled interchanges with neighboring areas. Because of a given power system loading is never constant and to ensure the quality of power supply, a load frequency controller is needed to maintain the system frequency at the desired nominal value. It is known that changes in real power affect mainly the system frequency and the input mechanical power to generators is used to control the frequency of the output electrical power. In a deregulated power system, each control area contains different kinds of uncertainties and various disturbances due to increased complexity, system modeling errors and changing power system structure. A well designed and operated power system should cope with changes in the load and with system disturbances and it should provide acceptable high level of power quality while maintaining both voltage and frequency within tolerable limits [1–3].

E-mail address: kassem_ahmed53@hotmail.com

Peer review under responsibility of Ain Shams University.
doi:10.1016/j.asej.2010.09.006

Production and hosting by Elsevier

During the last decades, various control strategies for LFC have been proposed [1–10]. This extensive research is due to the fact that LFC constitutes an important function on power system operation where the main objective is to regulate the output power of each generator at prescribed levels while keeping the frequency fluctuations within pre-defined limits. Robust adaptive control schemes have been developed [4–7] to deal with changes in system parametric under LFC strategies. A different algorithm has been presented in [8] to improve the performance of multi-area power systems. Viewing a multi-area power system under LFC as a decentralized control design for a multi-input multi-output system, it has been shown in [9] that a group of local controllers with tuning parameters can guarantee the overall system stability and performance. The result reported in [1,2] demonstrates clearly the importance of robustness and stability issues in LFC design. In addition, several practical points have been addressed in [5,10] which include recent technology used by vertically integrated utilities, augmentation of filtered area control error with LFC schemes and hybrid LFC that encompasses an independent system operator and bilateral LFC.

The applications of artificial neural networks, genetic algorithms, fuzzy logic and optimal control to LFC have been reported in [3–10].

Predictive control is now widely used in industry and a large number of implementation algorithms. Most of the control algorithms use an explicit process model to predict the future behavior of a plant and because of this, the term model predictive control (MPC) is often utilized [11–13]. The most important advantage of the MPC technology comes from the process model itself, which allows the controller to deal with an exact replica of the real process dynamics, implying a much better control quality. The inclusion of the constraints is the feature that most clearly distinguishes MPC from other process control techniques, leading to a tighter control and a more reliable controller. Another important characteristic, which contributes to the success of the MPC technology, is that the MPC algorithms consider plant behavior over a future horizon in time. Thus, the effects of both feedforward and feedback disturbances can be anticipated and eliminated, which permits the controller to drive the process output more closely to the reference trajectory.

Several versions of MPC techniques are Model Algorithmic Control (MAC) [14], Dynamic Matrix Control (DMC) [15], and Internal Model Control (IMC) [16]. Although the above techniques differ from each other in some details, they are fundamentally the same, because all of them are based on linear process modelling.

The neural network model predictive control (NN-MPC) is another typical and straightforward application of neural networks to nonlinear control. When a neural network is combined with MPC approach, it is used as a forward process model for the prediction of process output [17,18]. Neural model predictive control has been applied on process control as chemical [19] and industry [18] applications. But, applying MPC on power system stability and control is still very slightly [20].

The main objective of this study is to investigate the application of neural model predictive controller on the load frequency control and inter area tie-power control problem for a multi-area power system. The system is modeled and the NN-MPC is designed and applied on the system. A comparison between the proposed NN-MPC and a FLC is presented at different conditions and evaluated. The feasibility and effectiveness of the LFC together with the proposed neural model predictive controller have been demonstrated through computer simulations. Simulation results have proved that the proposed controller can give better overall performance. Simulation results show also that the NN-MPC gives promising results.

2. Two-area load-frequency control model

Fig. 1 shows a block diagram of the ith area of an n-area power system. Because of small changes in the load are expected during normal operation, a linearized area model can be used for the load-frequency control. The following one area equivalent model for the system is adopted.

The system investigated comprises an interconnection of two areas load frequency control. The block diagram of two areas load frequency control model is shown in Fig. 2. The model equations of two areas load frequency control can be written as follows [21]:

$$\Delta\dot{P}_{G1} = \frac{-1}{T_{G1}}\Delta P_{G1} + \frac{-1}{R_1 T_{G1}}\Delta f_1 + \frac{1}{T_{G1}}u_1 \tag{1}$$

$$\Delta\dot{P}_{T1} = \frac{1}{T_{T1}}\Delta P_{G1} + \frac{-1}{T_{T1}}\Delta P_{T1} \tag{2}$$

$$\Delta\dot{f}_1 = \frac{K_{p1}}{T_{p1}}\Delta P_{T1} + \frac{-1}{T_{p1}}\Delta f_1 - \frac{K_{p1}}{T_{p1}}\Delta P_{tie} - \frac{K_{p1}}{T_{p1}}\Delta P_{d1} \tag{3}$$

$$\Delta\dot{P}_{tie} = T_{12}\Delta f_1 - T_{12}\Delta f_2 \tag{4}$$

$$\Delta\dot{P}_{G2} = \frac{-1}{T_{G2}}\Delta P_{G2} + \frac{-1}{R_2 T_{G2}}\Delta f_2 + \frac{1}{T_{G2}}u_2 \tag{5}$$

$$\Delta\dot{P}_{T2} = \frac{1}{T_{T2}}\Delta P_{G2} + \frac{-1}{T_{T2}}\Delta P_{T2} \tag{6}$$

$$\Delta\dot{f}_2 = \frac{K_{p2}}{T_{p2}}\Delta P_{T2} - \frac{1}{T_{p2}}\Delta f_2 - \frac{a_{12}K_{p2}}{T_{p2}}\Delta P_{tie} - \frac{K_{p2}}{T_{p2}}\Delta P_{d2} \tag{7}$$

where

Δf_i = the incremental frequency deviation for the ith area;
ΔP_{di} = the incremental change in load demand for the ith area;
ΔP_{tie} = the incremental change in tie-line power;
ΔP_{Gi} = the incremental change in governor position for the ith area;
ΔP_{Ti} = the incremental change in power generation level for the ith area;
B_i = the bias constant for the ith area;
T_{Gi} = the governor time constant for the ith area;
T_{Ti} = the turbine time constant for the ith area;
K_{pi} = power system gain for the ith area;
T_{pi} = power system time constant for the ith area;
T_{ij} = the synchronizing constant between the ith and jth area;
R_i = gain of speed droop feedback loop for the ith area;
ACE_i = area control error of the ith area;
u_i = control input of the ith area.

The two areas power system can be written in state-space form as follows:

$$\dot{x} = Ax + Bu + \delta d \tag{8}$$

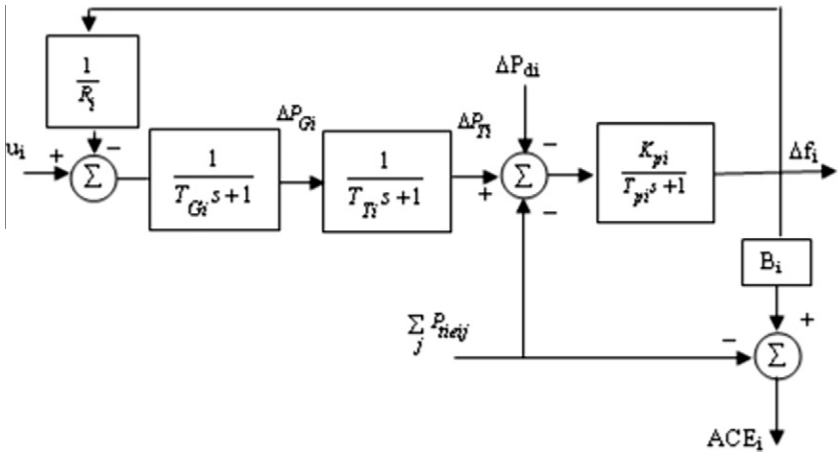

Figure 1 Block diagram of the *i*th area power system.

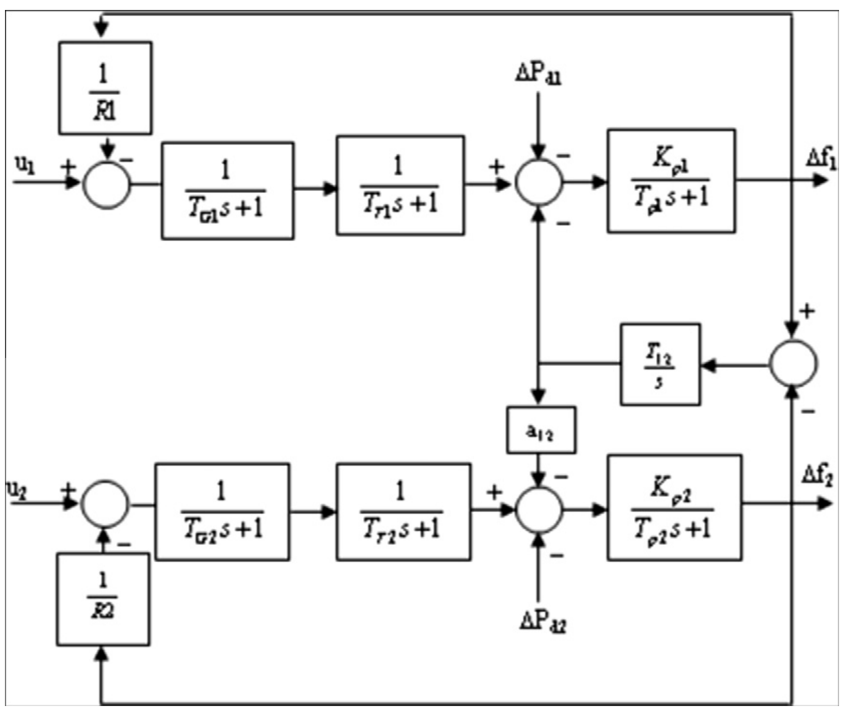

Figure 2 Two-area load frequency control system.

where

$x = [\Delta P_{G1} \quad \Delta P_{T1} \quad \Delta f_1 \quad \Delta P_{tie} \quad \Delta P_{G2} \quad \Delta P_{T2} \quad \Delta f_2]^T$,

$u = [u_1 \quad u_2]^T, \quad d = [\Delta P_{d1} \quad \Delta P_{d2}]^T$

$$A = \begin{bmatrix} \frac{-1}{T_{G1}} & 0 & \frac{-1}{R_1 T_{G1}} & 0 & 0 & 0 & 0 \\ \frac{1}{T_{T1}} & \frac{-1}{T_{T1}} & 0 & 0 & 0 & 0 & 0 \\ 0 & \frac{K_{p1}}{T_{p1}} & \frac{-1}{T_{p1}} & \frac{-K_{p1}}{T_{p1}} & 0 & 0 & 0 \\ 0 & 0 & T_{12} & 0 & 0 & 0 & -T_{12} \\ 0 & 0 & 0 & 0 & \frac{-1}{T_{G2}} & 0 & \frac{-1}{R_2 T_{G2}} \\ 0 & 0 & 0 & 0 & \frac{1}{T_{T2}} & \frac{-1}{T_{T2}} & 0 \\ 0 & 0 & 0 & \frac{-a_{12} K_{p2}}{T_{p2}} & 0 & \frac{K_{p2}}{T_{p2}} & \frac{-1}{T_{p2}} \end{bmatrix},$$

$$B = \begin{bmatrix} \frac{1}{T_{G1}} & 0 & 0 & 0 & 0 & 0 & 0 \\ 0 & 0 & 0 & 0 & \frac{1}{T_{G2}} & 0 & 0 \end{bmatrix}^T,$$

$$\delta = \begin{bmatrix} 0 & 0 & -\frac{K_{p1}}{T_{p1}} & 0 & 0 & 0 & 0 \\ 0 & 0 & 0 & 0 & 0 & 0 & -\frac{K_{p2}}{T_{p2}} \end{bmatrix}^T$$

3. Model based predictive control (MBPC)

MBPC is a name of several different control techniques. All are associated with the same idea. The prediction is based on the model of the process, as it is shown in Fig. 3.

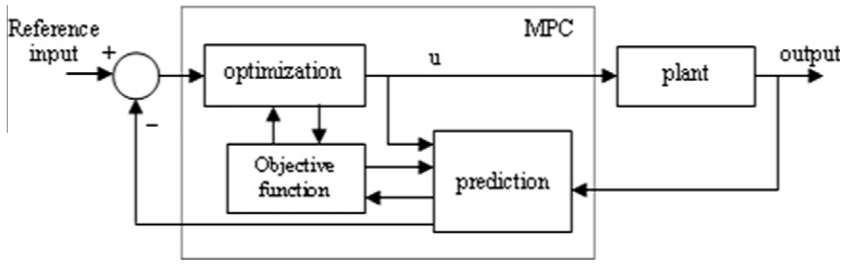

Figure 3 Classical model-based predictive control scheme.

The target of the model-based predictive control is to predict the future behaviour of the process over a certain horizon using the dynamic model and obtaining the control actions to minimize a certain criterion, generally [13]:

$$J = \sum_{k=N_1}^{N_2} (M(t+k) - Y_m(t+k))^2 + \sum_{k=1}^{N_u} (\lambda_k \Delta U_n(t+k))^2 \qquad (9)$$

Signals $M(k + t)$, $Y_m(k + t)$, $U_n(k + t)$ are the t-step ahead predictions of the process output, the reference trajectory and the control input, respectively. The values N_1 and N_2 are the minimal and maximal prediction horizon of the controlled output, and N_u is the prediction horizon of the control input. The value of N_2 should cover the important part of the step response curve. The use of the control horizon N_u reduces the computational load of the method. The parameter λ represents the weight of the control signal. At each sampling period only the first control signal of the calculated sequence is applied to the controlled process. At the next sampling time the procedure is repeated. This is known as the receding horizon concept.

The controller consists of the plant model and the optimization block. Eq. (9) is used in combination with the input and output constraints:

$$u_{\min} \leqslant u_i \leqslant u_{\max}, \quad i = 0, \ldots, N_2 - 1$$
$$\Delta u_{\min} \leqslant \Delta u_i \leqslant \Delta u_{\max}, \quad i = 0, \ldots, N_2 - 1$$
$$y_{\min} \leqslant y_i \leqslant y_{\max}, \quad i = 1, \ldots, N_2$$

The ability to handle constraints is one of the key properties of MBPC and also causes its spread, use, and popularity in industry. MBPC algorithms are reported to be very versatile and robust in process control applications.

4. Neural network predictive control

Neural networks have been applied very successfully in the identification and control of dynamic systems. The universal approximation capabilities of the multilayer perceptron (MLP) make it a popular choice for modelling of nonlinear systems and for implementing of nonlinear controllers. The use of a neural network for process modelling is shown in Fig. 4. The unknown function may correspond to a controlled system, and the neural network is the identified plant model. Two-layer networks, with sigmoid transfer functions in the hidden layer and linear transfer functions in the output layer, are universal approximators.

The prediction error between the plant output and the neural network output is used as the neural network training signal. The neural network plant model uses previous inputs and

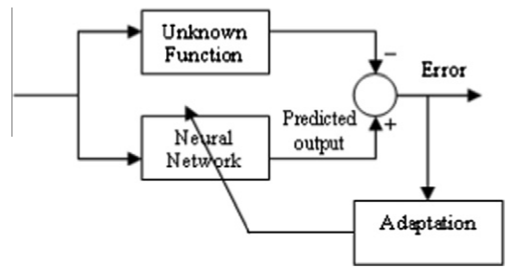

Figure 4 Neural network as a function approximator.

previous plant outputs to predict future values of the plant output. The structure of the neural network plant model is given in Fig. 5, where $u(t)$ is the system input, $y_p(t)$ is the plant output, $y_m(t)$ is the neural network model plant output, the blocks labelled TDL are tapped delay lines that store previous values of the input signal, $IW^{i,\,j}$ is the weight matrix from the input j to the layer i. $LW^{i,j}$ is the weight matrix from the layer j to the layer i.

This network can be trained off-line in batch mode, using data collected from the operation of the plant. The procedure for selecting the network parameters is called training the network. The Levenberg–Marquardt (LM) algorithm is very efficient for training. The LM algorithm is an iterative technique that locates the minimum of a function that is expressed as the sum of squares of nonlinear functions. It has become a standard technique for nonlinear least-squares problems and can be thought of as a combination of steepest descent and the Gauss–Newton method [22–25].

When the current solution is far from the correct one, the algorithm behaves like a steepest descent method: slow, but guaranteed to converge. When the current solution is close to the correct solution, it becomes a Gauss–Newton method.

Let f be an assumed functional relation which maps a parameter vector $P \in R^m$ to an estimated measurement vector $\hat{x} = f(p)$, $\hat{x} \in R^n$. An initial parameter estimate p_o and a measured vector $\boldsymbol{x}$ are provided, and it is desired to find the vector $\hat{p}$ that best satisfies the functional relation f, i.e. minimizes the squared distance $e^T e$ with $e = x - \hat{x}$. The basis of the LM algorithm is a linear approximation to f in the neighbourhood of p. For a small $\|\delta_p\|$, a Taylor series expansion leads to the approximation $f(P + \delta_p) \approx f(P) + J\delta_p$ where $\boldsymbol{J}$ is the Jacobi matrix $\frac{\partial f(P)}{\partial P}$. Like all non-linear optimization methods, LM is iterative: initiated at the starting point p_o, the method produces a series of vectors $\mathbf{p}_1, \mathbf{p}_2, \ldots,$ that converge towards a local minimizer $\hat{p}$ for f. Hence, at each step, it is required to find the δ_p that minimizes the quantity $\|e - J\delta_p\|$. The sought δ_p is thus the solution of a linear least-square problem: the minimum is attained when

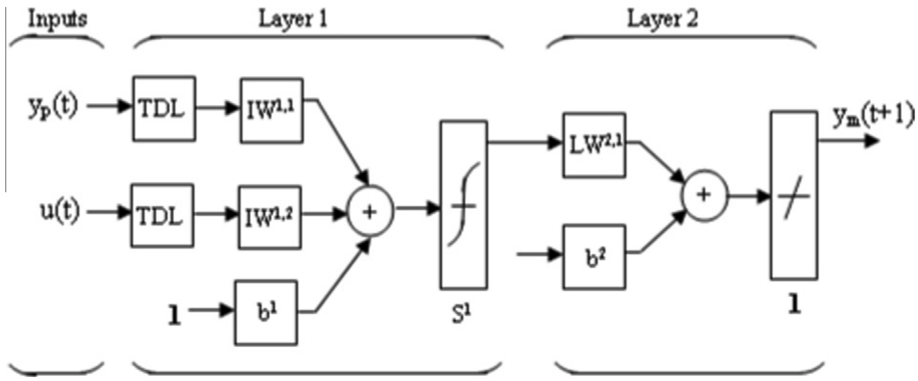

Figure 5 Structure of the neural network plant model.

$J\delta_p - e$ is orthogonal to the column space of **J**. This leads to $J^T(J\delta_p - e) = 0$, which yields δ_p as the solution of the normal equations:

$$J^TJ\delta_p = J^Te \tag{10}$$

The matrix J^TJ in the left hand side of Eq. (10) is the approximate Hessian, i.e. an approximation to the matrix of second order derivatives. The LM method actually solves a slight variation of Eq. (10), known as the augmented normal equations $N\delta_p = J^Te$, here the off-diagonal elements of N are identical to the corresponding elements of J^TJ and the diagonal elements are given by $N_{ii} = \mu + [J^TJ]_{ii}$ for some $\mu > 0$. The strategy of altering the diagonal elements of J^TJ is damping and μ is referred to the damping term. If the updated parameter vector $p + \delta_p$ with δ_p computed from Eq. (10) leads to a reduction of the error e, the update is accepted and the process repeats with a decreased damping term. Otherwise, the damping term is increased, the augmented normal equations are solved again and the process iterates until a value of δ_p that decreases error is found.

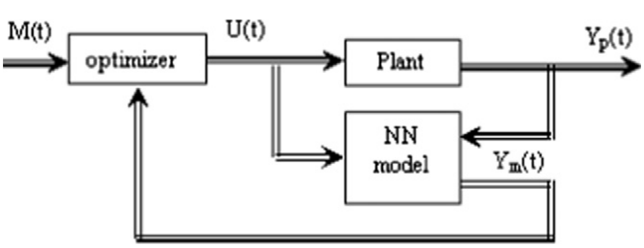

Figure 6 Multivariable NN-MPC control strategy.

In LM, the damping term is adjusted at each iteration to assure a reduction in the error e. The LM algorithm terminates when at least one of the following conditions is met:

1. The magnitude of the gradient of e^Te, i.e. J^Te in the right hand side of Eq. (10), drops below a threshold ϵ_1.
2. The relative change in the magnitude of δ_p drops below a threshold ϵ_2.
3. The error e^Te drops below a threshold ϵ_3.
4. A maximum number of iterations k_{max} is completed.

If a covariance matrix Σ for the measured vector $\boldsymbol{x}$ is available, the minimum is found by solving a weighted least squares problem defined by the weighted normal equations:

$$J^T\Sigma J\delta_p = J^T\Sigma e \tag{11}$$

Model predictive control using a neural network model for single-input, single-output systems has been studied by a few researchers and is outlined [26]. For multivariable systems, the neural network MPC strategy was described using three fixed MLP models [27]. The same strategy is used in our system using two MLP models with an adaptive model as shown in Fig. 6.

5. Fuzzy logic control

FLC operates in the same way as a human operator does. It performs the same actions by adjusting the input signal looking at only the system output. The fuzzy logic control approach consists of three stages, namely fuzzification, fuzzy control rules engine, and defuzzification as depicted in Fig. 7. To design the fuzzy logic load frequency controller, the input signals are the

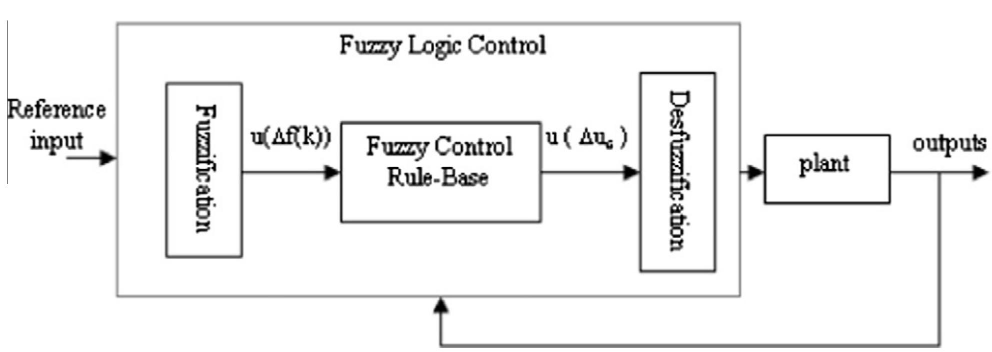

Figure 7 Three-stage of fuzzy logic controller.

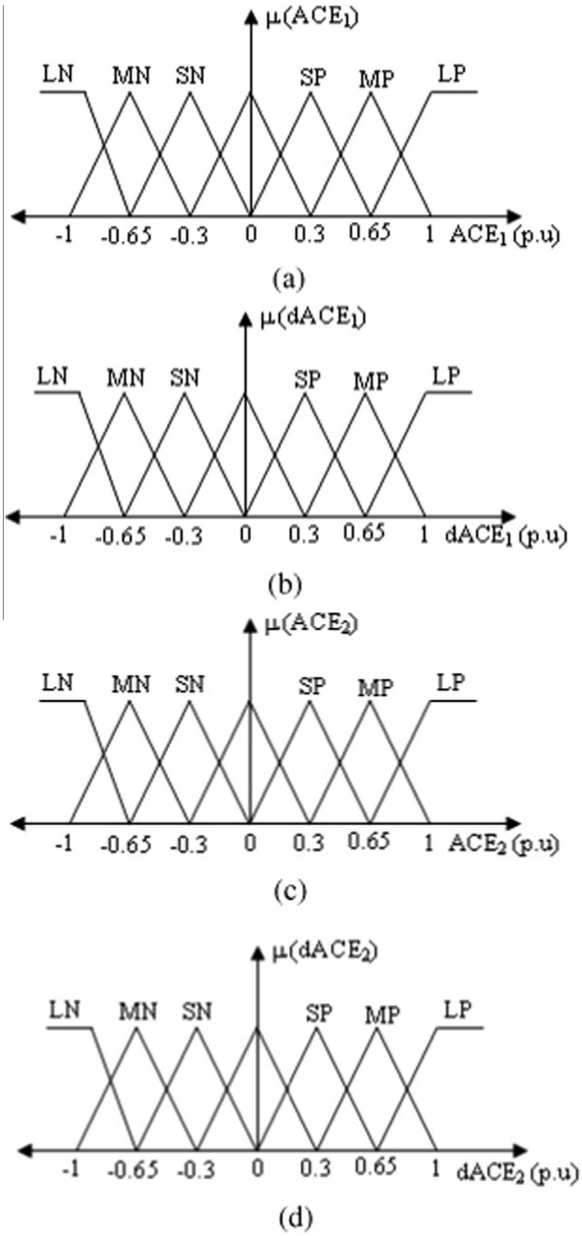

Figure 8 Membership functions. (a) Area one control error, (b) variation in area one control error, (c) area two control error, and (d) variation in area two control error.

area control error deviation at sampling time and its change in both area one and area two. While, its output signal is the change of control signal $\Delta U(k)$. Fig. 7 shows the fuzzy logic control system with the plant. While the fuzzy membership function signal is described in Fig. 8, and fuzzy control rules are illustrated in Table 1. The membership function shapes of error and derivative error and the controller outputs are chosen to be identical with triangular function for fuzzy logic control. However, this horizontal axis range takes different values because of optimizing controller.

6. Implementation scheme

The objective of this control is to regulate the terminal frequency at the area output and minimize the deviation between the actual and reference area control error (ACE), the block diagrams of LFC with the proposed NN-MPC and FLC are shown in Figs. 9 and 10 respectively. The cost function of Eq. (9) will have the following form for the proposed system:

Table 1 Fuzzy logic control rules (Δf).

ΔACE	$d\Delta ACE$						
	LN	MN	SN	Z	SP	MP	LP
LN	LP	LP	LP	MP	MP	SP	Z
MN	LP	MP	MP	MP	SP	Z	SN
SN	LP	MP	SP	SP	Z	SN	MN
Z	MP	MP	SP	Z	SN	MN	MN
SP	MP	SP	Z	SN	SN	MN	LN
MP	SP	Z	SN	MN	MN	MN	LN
LP	Z	SN	MN	MN	LN	LN	LN

LN: large negative membership function; MN: medium negative; SN: small negative; Z: zero; SP: small positive; MP: medium positive; LP: large positive.

$$J = \sum_{k=N_1}^{N_2} \left(ACE(t+k) - ACE_{pred}(t+k)\right)^2 + \sum_{k=1}^{N_u} \left(\lambda_k \Delta ACR_{ref}(t+k)\right)^2 \quad (12)$$

where

$$\Delta ACR_{ref} = ACR_{ref}(t+k) - ACR_{ref}(t+k-1)$$

the constraints are chosen such that, the area output frequency and tie power are normalized to be 1, corresponds to output frequency and tie power. Thus,

$$ACR_{ref} - \varepsilon \leqslant u \leqslant ACR_{ref} + \varepsilon.$$

7. Digital simulation results

The controller using a neural network model to predict future LFC responses and potential control signals is designed. Then, an optimization algorithm related to Eq. (12) computes the control signals that optimize future plant performance. The neural network plant model was trained using the Levenberg–Marquardt algorithm. The training data were obtained from the model of the LFC (1–7). The used model predictive control method was based on the receding horizon technique. The neural network model predicted the plant response over a specified time horizon. The predictions were used by a numerical optimization program to determine the control signal that minimizes performance criterion over the specified horizon. The controller was implemented using Matlab/Simulink with the following constraints and parameters values:

$$N_1 = [1 \quad 1], \quad N_2 = [7 \quad 6], \quad N_u = [2 \quad 3] \quad \text{and} \quad \lambda = [0.05 \quad 0.08]$$

The constraints on the states are chosen such that to guarantee signals stay at physically reasonable values as follows:

$$x_{\min} \leqslant \begin{pmatrix} \Delta f_1 \\ \Delta f_2 \\ \Delta P_{ti} \end{pmatrix} \leqslant x_{\max}$$

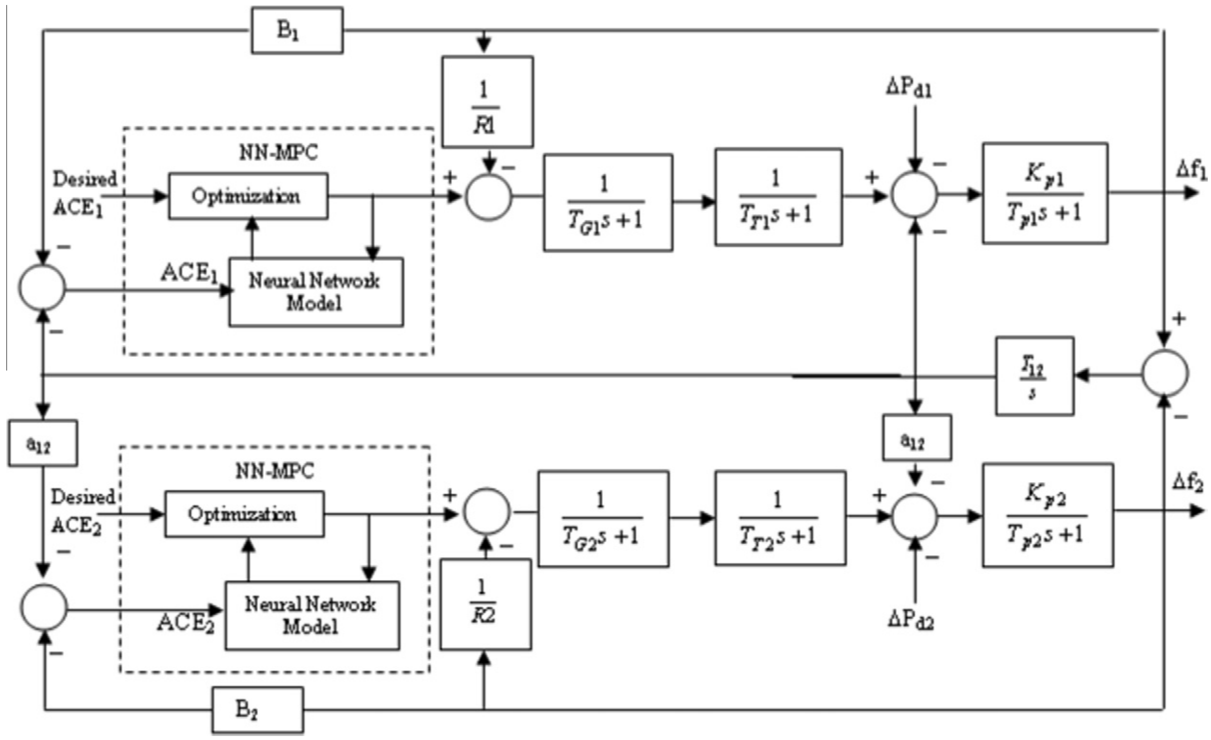

Figure 9 The proposed NN-MPC of the two-area load frequency control power system.

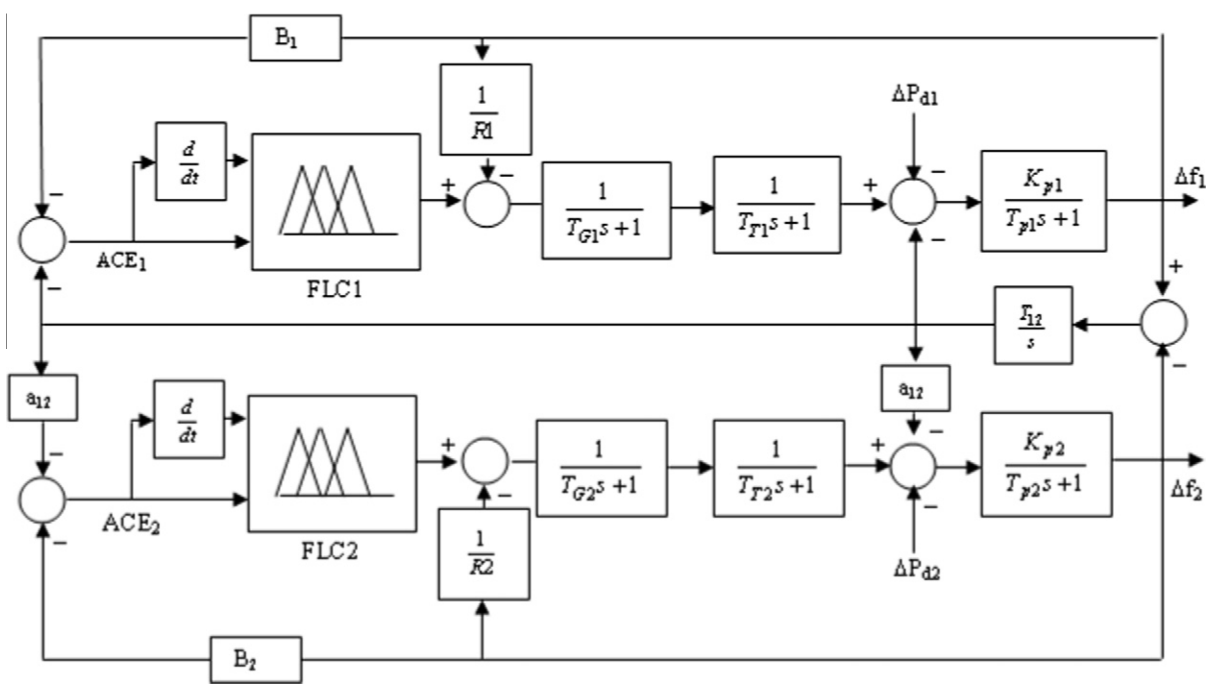

Figure 10 The block diagram of FLC of the two-area load frequency control power system.

where

$$x_{\min} = \begin{pmatrix} -0.05 \\ -0.05 \\ -0.03 \end{pmatrix}, \quad x_{\max} = \begin{pmatrix} 0.05 \\ 0.05 \\ 0.03 \end{pmatrix}$$

A comparison between the power system responses using the fuzzy logic controller and the proposed NN-MPC are evaluated. The investigated system parameters are [28]:

$f_o = 60$ Hz, $R_1 = R_2 = 2.4$ Hz/per unit MW, $T_{G_1} = T_{G_2} = 0.08$ s, $T_{T_1} = T_{T_2} = 0.3$ s, $B_1 = B_2 = 0.4$ MW/Hz, $T_{p_1} = T_{p_2} = 20$, $a_{12} = -1$; $K_{p_1} = 120$; $K_{p_2} = 120$; $T_{12} = 0.545$ MW.

Fig. 11 displays the frequency deviation response of area-1 due to 0.05 p.u. load disturbance in area-1 of the two-area power system with FLC and proposed NN-MPC. Fig. 12 shows the frequency deviation response of area-2 due to 0.05 p.u. load disturbance in area-1 of the two-area power system with FLC and proposed NN-MPC. Fig. 13 shows the tie-line power deviation response due to 0.05 p.u. load disturbance in area-1 of the two-area power system with FLC and proposed NN-MPC. Fig. 14 shows the frequency deviation response of area-1 due to 0.05 p.u. load disturbance in area-2 of the two-area power system with FLC and proposed NN-MPC at 30% increase in regulators R1 and R2. Also, Fig. 15 depicts the frequency deviation response of area-2 due to 0.05 p.u. load disturbance in area-2 of the two-area power system with FLC and proposed NN-MPC at 30% increase in regulators R1 and R2. Fig. 15 depicts the tie-line power deviation response due to 0.05 p.u. load disturbance in area-2 of the two-area power system with FLC and proposed NN-MPC at 30% increase in regulators R1 and R2. The maximum over shoot (max. O. S.) and the settling time (T_s) for the FLC with the proposed NN-MPC and FLC are shown in Table 2.

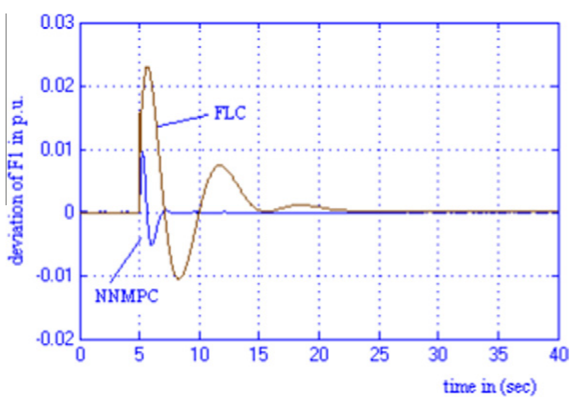

Figure 11 Frequency deviation response of area-1 due to 0.05 p.u. load disturbance in area-1 of the two-area power system with FLC and proposed NN-MPC.

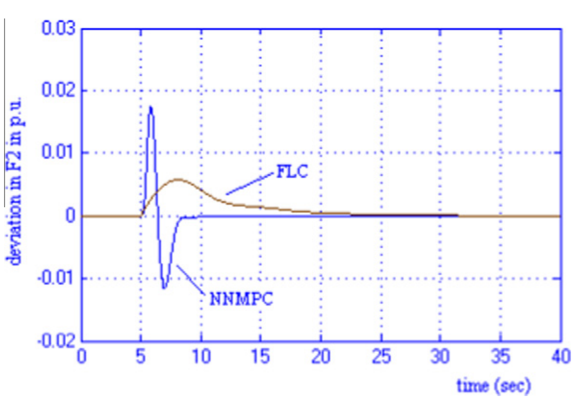

Figure 12 Frequency deviation response of area-2 due to 0.05 p.u. load disturbance in area-1 of the two-area power system with FLC and proposed NN-MPC.

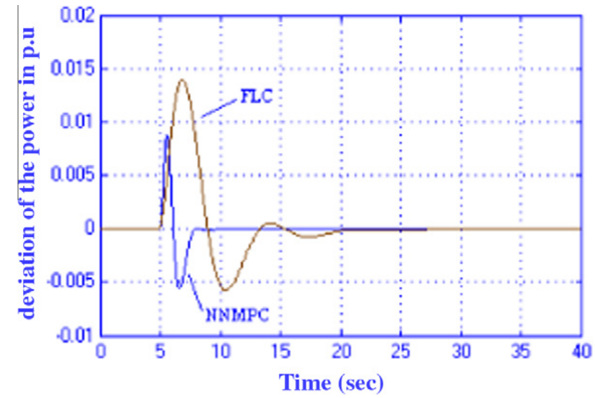

Figure 13 Tie-line power deviation response due to 0.05 p.u. load disturbance in area-1 of the two-area power system with FLC and proposed NN-MPC.

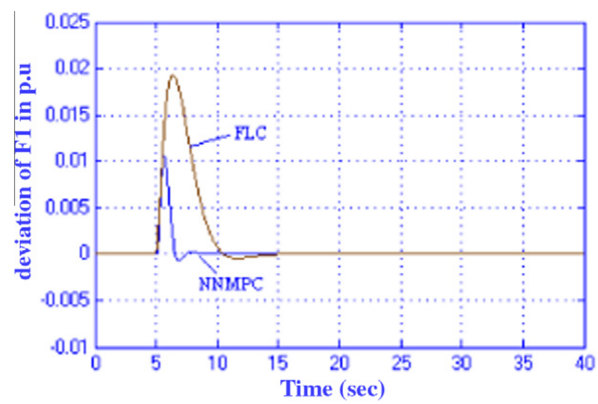

Figure 14 Frequency deviation response of area-1 due to 0.05 p.u. load disturbance in area-2 of the two-area power system with FLC and proposed NN-MPC at 30% increase in regulators R1 and R2.

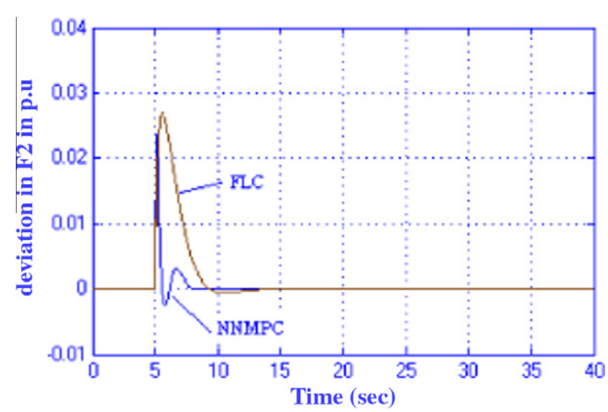

Figure 15 Frequency deviation response of area-2 due to 0.05 p.u. load disturbance in area-2 of the two-area power system with and without fuzzy logic and proposed NN-MPC at 30% increase in regulators R1 and R2.

Table 2 The settling time and maximum over shoot calculation with FLC and NN-MPC.

	5% Disturbance in area No. 1				5% Disturbance in area No. 2			
	NN-MPC		FLC		NN-MPC		FLC	
	T_s (s)	Max. O. S. (p.u.)	T_s (s)	Max. O. S. (p.u.)	T_s (s)	Max. O. S. (p.u.)	T_s (s)	Max. O. S. (p.u.)
Δf_1	2.5	0.01	16	0.024	2.5	0.01	8	0.019
Δf_2	3	0.018	13	0.006	3	0.013	6	0.028
ΔP_{tie}	3	0.0008	15	0.013	3	0.0025	6	0.004

T_s is the the settling time in seconds.

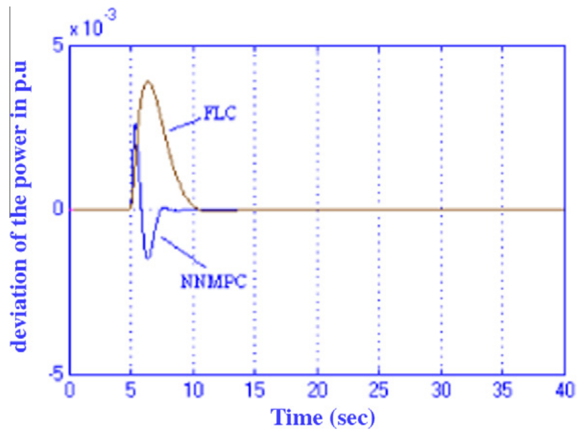

Figure 16 Tie-line power deviation response due to 0.05 p.u. load disturbance in area-2 of the two-area power system with FLC and proposed NN-MPC at 30% increase in regulators R1 and R2.

8. Discussions

The fuzzy rules matrix for fuzzy logic controller is developed, considering 49 rules as in Table 1 by using Triangular membership functions. Moreover, a NN-MPC is designed and optimized based on power system model, control horizon and prediction horizon. Various transient response curves of Δf_1, Δf_2, $\Delta P_{tie\text{-}line}$ are obtained and comparative studies have been done. The following points may be noted (see Fig. 16):

1. From Figs. 11–16 and Table 2, the frequency deviation responses based on proposed NN-MPC is better than fuzzy logic control in terms of fast response and small maximum overshoot.
2. The tie line power is also fast decreased in case of NN-MPC than FLC.
3. The performance of the NN-MPC is shown in Figs. 11–16 and Table 2 shows that NN-MPC is effective enough to eliminate the mechanical oscillation after 3 s.
4. The performance of the FLC is shown in Figs. 11–16 and Table 2 shows that FLC is not effective enough to eliminate the mechanical oscillation after 16 s.
5. In order to have a better prediction of the future behavior of the plant, the prediction horizon should be more than the period of the system.
6. Neural network model predictive control has been shown to be successful in addressing many large scale non-linear control problems and therefore is better considering for stabilization of a power system.

9. Conclusions

The scope of this paper is to investigate the potential improvements that can be achieved using neural predictive methodologies for the load frequency control of two area interconnected power system. To validate the effectiveness of the proposed controller a comparison among the fuzzy logic controller and the proposed NN-MPC controller is obtained. Both the proposed NN-MPC and FLC with the LFC interconnected power system is tested through load disturbances. From the simulations, it is concluded that the proposed controller is robust and gives good transient response as well as steady-state performance and it is robust to variations in system parameter changes. Also from the simulation results it is concluded that the proposed control approach achieves better control results than a fuzzy logic control.

References

[1] Wang Y, Hill DJ, Guo G. Robust decentralized control for multimachine power system. IEEE Trans Circuits Syst: Fund Theory Appl 1998;45(3).

[2] Shayeghi H. Robust modified GA based multi-stage fuzzy LFC. Energy Convers Manage 2007;48:1656–70.

[3] Shayegi H, Shayanfar HA, Malik OP. Robust decentralized neural networks based LFC in a deregulated power system. Electr Power Syst Res 2007;77:241–51.

[4] Pan CT, Liaw CM. An adaptive control for power system LFC. IEEE Trans Power Syst 1989;4(1):122–8.

[5] Talaq J, Al-basri H. Adaptive fuzzy gain scheduling for LFC. IEEE Trans Power Syst 1999;14(1):145–50.

[6] Kocaarslan İlhan, Çam Ertuğrul. Fuzzy logic controller in interconnected electrical power systems for load-frequency control. Int J Electr Power Energy Syst 2005;27(8):542–9.

[7] Anand B, Ebenezer Jeyakumar A. Load frequency control with fuzzy logic controller considering non-linearities and boiler dynamics. ICGST-ACSE J 2009;8(III).

[8] Šijak Tomislav, Kulja Ognjen, Kulja Ljubomir, Tešnjak Sejid. Design of fuzzy regulator for power system secondary load frequency control. In: Proceedings of the 10th Mediterranean conference on control and automation – MED2002, Lisbon, Portugal, 2002.

[9] Çam Ertuğrul. Application of fuzzy logic for load frequency control of hydro electrical power plants. Energy Convers Manage 2007;48(4):1281–8.

[10] Çam Ertu rul, Kocaarslan Ihan. Load frequency control in two area power systems using fuzzy logic controller. Energy Convers Manage 2005;46(2):233–43.

[11] Draeger A, Engel SH, Ranke H. Model predictive control using neural networks. IEEE Control Syst Mag 1995;15:61–6.

[12] Gomm JB, Evans JT, Williams D. Development and performance of a neural network predictive controller. Control Eng Pract 1997;5(1):49–60.
[13] Abad Frahani Shams, Nekouei MA, Nikzad Mehdi. Predictive control of a single link flexible joint robot based on neural network and feedback linearization. Aust J Basic Appl Sci 2009;3(3):2322–33.
[14] Richalet JA, Rault A, Testud JD, Papon J. Model predictive heuristic control: applications to an industrial process. Automatica 1978;14:413–28.
[15] Cutler CR, Ramaker BL. Dynamic matrix control – a computer control algorithm. In: Proc. of American Control Conf. WP5-B; 1980.
[16] Garcia CE, Morari M. Internal model control – I. A unifying review and some new results. Ind Eng Chem Process Des Dev 1982;21:308–23.
[17] Kuure-Kinsey M, Cutright R, Bequette BW. Computationally efficient neural predictive control based on a feedforward architecture. Ind Eng Chem Res 2006;45:8575–82.
[18] Kittisupakorn Paisan, Thitiyasook Piyanuch, Hussain MA, Daosud Wachira. Neural network based model predictive control for a steel pickling process. J Process Control 2009;19(4):579–90.
[19] Kalman Nagy Zoltan. Model based control of a yeast fermentation bioreactor using optimally designed artificial neural networks. Chem Eng J 2007;127(1–3):95–109.
[20] Papafotiou Georgios, Geyer Tobias, Morari Manfred. A hybrid model predictive control approach to the direct torque control problem of induction motors. Int J Robust Nonlinear Control 2007;17:1572–89.
[21] Taher Seyed Abbas, Hematti Reza, Abdolalipour Ali, Tabei Seyed Hadi. Optimal decentralized load frequency control using HPSO algorithms in deregulated power systems. Amer J Appl Sci 2008;5(9):1167–74.
[22] De Pierro R Alvaro, Wei Musheng. Some new properties of the equality constrained and weighted least squares problem. Linear Algebra Appl. 2000;320(1-3):145–65.
[23] Stewart GW. On the weighting method for least squares problems with linear equality constraints. BIT Numer Math 1997;37(4):961–7.
[24] Biegler-Konig F, Barmann F. A learning algorithm for multilayered neural networks based on linear least squares problems. Neural Networks 1993;6(1):127–31.
[25] Lawson CL, Hanson RJ. Solving least squares problems. Prentice-Hall; 1987.
[26] Hunt KJ, Sbarbaro D, Zbikowski R, Gawthrop PJ. Neural networks for control systems – a survey. Automatica (J IFAC) 1992;28(6):1083–112.
[27] Li Ning, Li Shao-Yuan, Xi Yu-Geng. Multi-model predictive control based on the Takagi–Sugeno fuzzy models: a case study. Informatics Comput Sci Intell Syst Appl 2004;165(3-4):247–63.
[28] El-Sherbiny MK, El-Saady G, Youssef Ali M. Efficient fuzzy logic load-frequency controller. Energy Convers Manage J 2002;43:1853–63.

Dr. Ahmed M. Kassem is an assistant professor at Bini-Swief University, Faculty of Industrial Education, Control Department. His field of interest includes renewable energy, electric drives control, power system control and power electronics.